NANO LETTERS

Letter

pubs.acs.org/NanoLett

Demonstration of Zero Optical Backscattering from Single Nanoparticles

Steven Person,[†] Manish Jain,[†] Zachary Lapin,[‡,†] Juan Jose Sáenz,[§] Gary Wicks,[†] and Lukas Novotny*[,‡,†]

[†]Institute of Optics, University of Rochester, Rochester New York 14627, United States

[‡]Photonics Laboratory, ETH Zürich, 8093 Zürich, Switzerland

[§]Departamento de Física de la Materia Condensada, Instituto "Nicolás Cabrera" and Centro de Investigación en Física de la Materia Condensada (IFIMAC), Universidad Autónoma de Madrid, 28049-Madrid, Spain

Supporting Information

ABSTRACT: We present the first experimental demonstration of zero backscattering from nanoparticles at optical frequencies as originally discussed by Kerker et al. [Kerker, M.; Wang, D.; Giles, C. *J. Opt. Soc. A* **1983**, *73*, 765]. GaAs pillars were fabricated on a fused silica substrate and the spectrum of the backscattered radiation was measured in the wavelength range 600−1000 nm. Suppression of backscattering occurred at ∼725 nm, agreeing with calculations based on the discrete dipole approximation. Particles with zero backscattering provide new functionality for metamaterials and optical antennas.

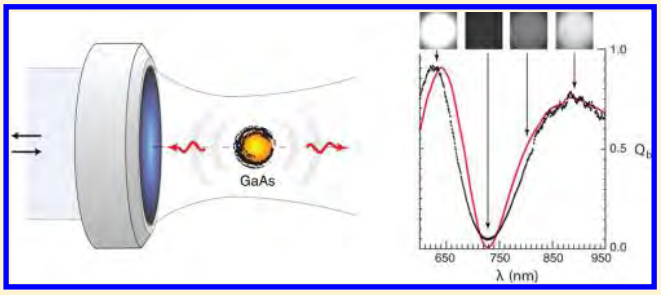

KEYWORDS: *Nanoparticles, scattering, metamaterials*

Nanofabrication techniques continue to fuel the search for structures that exhibit unique optical properties. Among these structures are optical antennas, which concentrate and direct light,[1] and metamaterials that can mimic optical constants not found in nature.[2,3] Optical antennas and metamaterials often capitalize on the plasmonic properties of metal nanostructures.[4,5] Plasmons, however, have large nonradiative losses that restrict practical applications to narrow frequency bands,[6] even if active gain media are employed.[7] Recently, alternative approaches using dielectric materials have been proposed for constructing optical antennas[8−11] and metamaterials.[12−14]

The optical properties of dielectric nanostructures are strongly influenced by the interaction of electric and magnetic Mie resonances. Thirty years ago, Kerker et al. showed that the backscattered light from spherical scatterers can be completely suppressed if the dielectric and magnetic properties of the scatterers are the same ($\varepsilon = \mu$).[15] A particle with these properties exhibits equal electric (a_n) and magnetic (b_n) multipole coefficients[16] that destructively interfere in the backward propagating direction (first Kerker condition). Until recently, zero backscattering at visible wavelengths has been a theoretical curiosity[17−19] due to the lack of magnetic materials ($\mu \neq 1$) in the optical regime.

Kerker's condition for zero backscattering is valid for any size spherical particle. For nanoparticles, however, the scattered field is sufficiently described by the electric (a_1) and magnetic (b_1) dipole terms of the Mie expansion.[20] In terms of a_1 and b_1 the electric and magnetic polarizabilities are defined as

$$\alpha_e = \frac{3i\varepsilon}{2k^3}a_1 \quad \alpha_m = \frac{3i}{2\mu k^3}b_1 \tag{1}$$

respectively, where $k = 2\pi n_m/\lambda$, with n_m being the refractive index of the surrounding medium and λ the vacuum wavelength. The two dipoles interfere constructively or destructively depending on their relative phase. In the backward direction the particle's scattering cross-section is

$$\sigma_b = 4\pi k^4 I_\alpha[1 + V_\alpha \cos(\pi - \Delta\phi_\alpha)] \tag{2}$$

where $I_\alpha = |\alpha_e/\varepsilon|^2 + |\mu\alpha_m|^2$ is the incoherent sum of the two dipoles, $\Delta\phi_\alpha$ is the phase difference between the dipoles, and V_α, given by

$$V_\alpha = \frac{2|\alpha_e/\varepsilon||\mu\alpha_m|}{I_\alpha} \tag{3}$$

controls the backscattering suppression. A minimum in the backscattered field will occur whenever the electric and magnetic dipoles are oscillating in phase ($\Delta\phi_\alpha = 0$). The minimum will be exactly zero if V_α is equal to one.

Note that the elimination of the backscattered field in eq 2 is valid even for nonmagnetic materials ($\mu = 1$) provided that the dipole approximation holds. This approximation requires dielectric nanoparticles with a large index of refraction ($n \sim 3-4$), such as silicon and germanium.[21,22] Recently, the electric

Received: February 7, 2013
Revised: February 27, 2013
Published: March 5, 2013

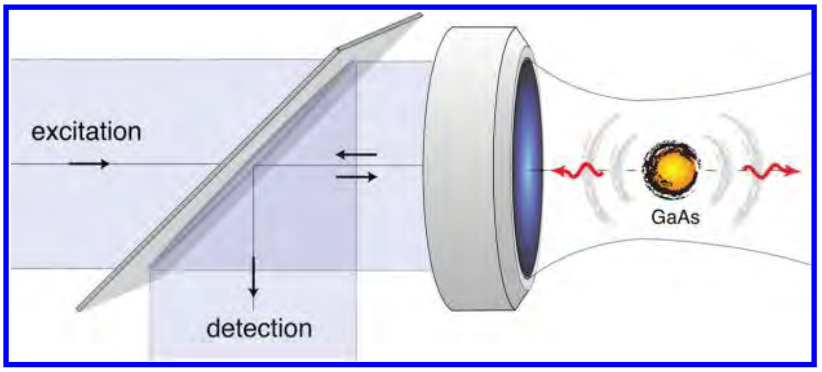

Figure 1. Illustration of the backscattering measurement. White light is weakly focused on a GaAs particle of radius ~90 nm. Backscattered light is separated by a 50/50 beamsplitter and sent to a spectrometer.

and magnetic dipole and quadrupole resonances have been experimentally measured for silicon spheres in the visible.[23−25] The large refractive index of these nanoparticles make them ideally suited for verifying Kerker's theoretical predictions.

In this Letter, we experimentally demonstrate the suppression of optical backscattering from dielectric nanoparticles, as predicted by Kerker.[15] A recent experiment has demonstrated suppressed backscattering at microwave frequencies,[26] however, a verification at optical wavelengths has not yet been performed. We chose GaAs as a scattering material due to its large index of refraction ($n \sim 3.6$) in the 600−1000 nm wavelength range.[27] The experimental arrangement is sketched in Figure 1: white light is weakly focused on a sample of well separated GaAs nanoparticles and the backscattered light is separated by a beamsplitter and directed on a spectrometer. Figure 2a is a plot of the extinction efficiency ($Q_{ext} = \sigma_{ext}/\pi r^2$)

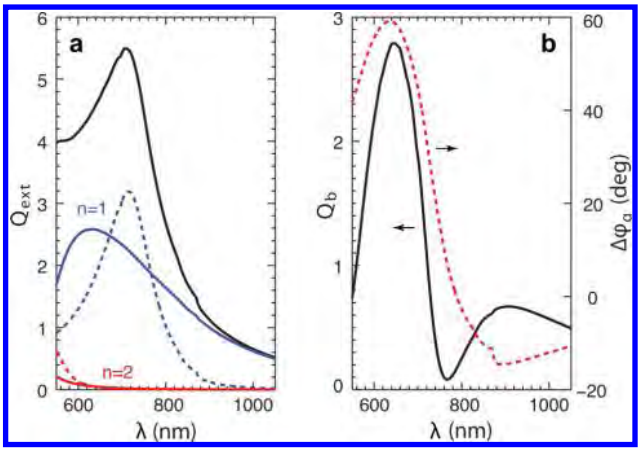

Figure 2. Mie theory calculations of a 90 nm radius sphere of GaAs embedded in a uniform medium of refractive index $n_m = 1.47$. (a) Electric (solid) and magnetic (dashed) dipole ($n = 1$) and quadrapole ($n = 2$) contributions to the total extinction efficiency (Q_{ext}). (b) Backscattering efficiency (Q_b) and phase difference ($\Delta\phi_\alpha$) between the electric and magnetic dipoles.

for a GaAs sphere of radius $r = 90$ nm immersed in a medium of index $n_m = 1.47$. The contributions of the dipole terms (a_1, b_1) and the quadrupole terms (a_2, b_2) of Q_{ext} are shown as separate curves. The curves show that for wavelengths longer than ~600 nm the electric and magnetic quadrupole terms can be neglected. The backscattering efficiency ($Q_b = \sigma_b/\pi r^2$) is plotted in Figure 2b. A minimum in Q_b is located at ~775 nm where the relative phase between the electric and magnetic dipoles crosses zero ($\Delta\phi_\alpha \sim 0$).

To measure backscattering from GaAs nanoparticles embedded in a uniform environment we implemented an epitaxial lift-off technique in conjunction with a water-bonding procedure to attach a high quality GaAs membrane (grown on a GaAs substrate) to a fused silica substrate.[28,29] Direct growth of GaAs on fused silica is avoided because it results in a high density of dislocations. Figure 3c illustrates the fabrication

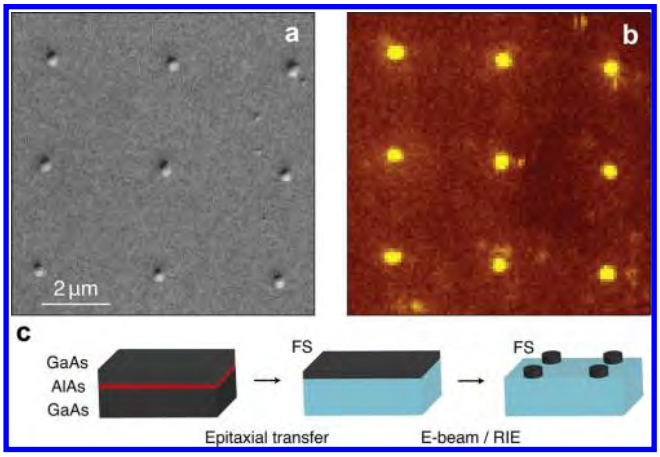

Figure 3. (a,b) Characterization of the fabricated GaAs nanoparticle sample. (a) SEM image of an array of GaAs pillars of radius $r \sim 90$ nm. (b) Confocal photoluminescence image of the same sample area. Wavelength of excitation laser: $\lambda = 532$ nm. Detection: $\lambda > 550$ nm. (c) Steps of the sample fabrication process showing the transfer of the GaAs epitaxial layer to a fused silica (FS) substrate and the generation of GaAs pillars with *e*-beam lithography and reactive-ion etching (RIE).

steps. Using molecular beam epitaxy (MBE), a 40 nm sacrificial layer of AlAs was deposited on a GaAs substrate. On top of the AlAs layer a 1 μm film of GaAs was grown. Using the epitaxial lift-off procedure, the 1 μm GaAs film was transferred to a fused silica substrate. The transferred GaAs film was initially reduced to a thickness of ~150 nm by reactive ion etching (RIE). An array of ~175 nm diameter discs was then patterned in a poly(methyl methacrylate) (PMMA) resist using *e*-beam lithography. After developing the resist, GaAs pillars were created by RIE. The leftover PMMA was removed with an additional oxygen plasma etch. Figure 3a shows a scanning electron microscope (SEM) image of the fabricated structures. To verify that no residual GaAs remained after etching, a

dx.doi.org/10.1021/nl4005018 | *Nano Lett.* 2013, 13, 1806−1809

confocal scanning image of the photoluminescence was taken with an excitation laser of λ = 532 nm. The confocal image in Figure 3b shows strong signal from the GaAs pillars with limited luminescence from the fused silica substrate.

Backscattering measurements were done using a standard inverted microscope with a fiber-coupled tungsten halogen white light source (see Figure 1). To create a uniform environment and eliminate any back-reflections index matching oil covered the top of the sample. The sample was broadly illuminated by weakly focusing the white light source through an oil immersion objective. The backscattered light was collected with the same objective and sent to either an avalanche photodiode (APD) or a spectrometer. A 10 nm bandpass filter was placed in front of the APD and the sample was scanned by a piezo positioning stage to form an image. Spectra of single GaAs pillars were acquired in the wavelength range of 600−1000 nm. The collection volume was limited either by the APD detector area or the spectrometer slit width. This ensured that light from only a single scatterer was detected even though the sample was broadly illuminated.

The recorded spectra and APD images were corrected for source spectrum nonuniformity, transmission losses, and detector efficiencies. A baseline spectrum $[I_{\mathrm{mirror}}(\lambda)]$ was recorded by replacing the sample with a mirror. Additionally, the background spectrum $[I_{\mathrm{bkg}}(\lambda)]$ measured on the fused silica substrate away from the GaAs pillars was subtracted. This background resulted from a slight refractive index mismatch between substrate and index-matching oil. The final backscattering efficiency is calculated as

$$Q_{\mathrm{b}}(\lambda) = \beta \frac{I_{\mathrm{meas}}(\lambda) - I_{\mathrm{bkg}}(\lambda)}{I_{\mathrm{mirror}}(\lambda)} \quad (4)$$

where I_{meas} is the recorded spectrum. The prefactor β is a calibration scaling factor.

Figure 4 shows the resulting backscattering efficiency recorded for a single GaAs pillar. The spectrum has a pronounced dip at ∼725 nm where the backscattered field is suppressed due to the interference between the electric and magnetic dipole components. Though the suppressed backscattered field is obvious, there are two notable differences in the spectral shape when comparing to the Mie theory calculation of Figure 2b. First, the scattering amplitude below ∼700 nm is suppressed and, second, the location of the minimum is blue-shifted. Both of the differences are attributed to the fact that the structure is a pillar rather than a sphere. Compared to a sphere of the same volume, a pillar with an aspect ratio (height/diameter) below one will have the location of the minimum blue shifted and the scattering peak to the left of the minimum suppressed (Supporting Information). The solid curve in Figure 4 is a simulation of the backscattered field of a GaAs pillar calculated using the discrete dipole approximation.[30] The simulated structure has a height of 137 nm and a diameter of 165 nm, which is within 10% of the initial design parameters. The sequence of images above Figure 4 are backscattering images with bandwidth of 10 nm and center wavelengths indicated by the arrows. At the location of the spectral minimum, the image of the scatterer fades into the background.

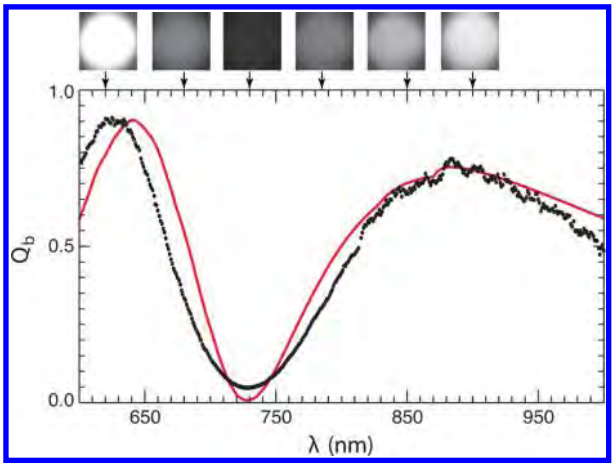

Figure 4. Backscattering spectrum from a single GaAs pillar. The black dotted curve is the measured spectrum and the red curve is the theoretical spectrum calculated using the discrete dipole approximation. The series of images above the graph are backscattering images of a GaAs pillar recorded with 10 nm bandpass filters at various center wavelengths.

In conclusion, we have shown the first experimental verification of Kerker's theoretical prediction of zero backscattering in the optical wavelength range. Using pillars, rather than spheres, slight shifts of the wavelength of minimum backscattering can be observed. This shift as well as the reshaping of the spectrum are reproduced with calculations based on the discrete dipole approximation. Understanding and verifying the response of single dielectric nanoparticles is crucial in any bottom-up nanofabrication technique. The remarkable properties of these particles with zero backscattering but significant light dispersion in forward direction suggest intriguing technological applications, for example, as light diffusing elements in solar cells. Using similar GaAs structures, experiments involving arrays of scatterers[31] or dielectric antennas manipulating magnetic dipoles[32,33] are possible.

After the first submission of this manuscript a related study has been published.[34] In this work, authors experimentally demonstrated Kerker's-type zero backward scattering by Si particled in the whole visible spectrum.

■ ASSOCIATED CONTENT

Supporting Information

Additional information is provided on scattering properties of cylinders and theoretical methods. This material is available free of charge via the Internet at http://pubs.acs.org.

■ AUTHOR INFORMATION

Corresponding Author

*E-mail: lnovotny@ethz.ch.

Notes

The authors declare no competing financial interest.

■ ACKNOWLEDGMENTS

This work is funded by the U.S. Department of Energy (Grant DE-FG02-01ER15204). J.J.S. acknowledges support from the Spanish Ministerio de Ciencia e Innovación through Consolider NanoLight (CSD2007-00046) and from the Comunidad de Madrid Microseres-CM (S2009/TIC-1476).

■ REFERENCES

(1) Bharadwaj, P.; Deutsch, B.; Novotny, L. *Adv. Opt. Photonics* **2009**, *1*, 438−483.
(2) Shalaev, V. M. *Nat. Photonics* **2007**, *1*, 41−48.
(3) Soukoulis, C. M.; Wegener, M. *Nat. Photonics* **2011**, *5*, 523−530.

(4) Schuller, J. A.; Barnard, E.; Cai, W.; Jun, Y. C.; White, J.; Brongersma, M. L. *Nat. Mater.* **2010**, *9*, 193−204.
(5) Kawata, S.; Inouye, Y.; Verma, P. *Nat. Photonics* **2009**, *3*, 388−394.
(6) Stockman, M. *Phys. Rev. Lett.* **2007**, *98*, 177404.
(7) Hess, O.; Pendry, J. B.; Maier, S. A.; Oulton, R. F.; Hamm, J. M.; Tsakmakidis, K. L. *Nat. Mater.* **2012**, *11*, 573−584.
(8) Schuller, J. A.; Brongersma, M. L. *Opt. Express* **2009**, *17*, 24084−24095.
(9) Rolly, B.; Stout, B.; Bonod, N. *Opt. Express* **2012**, *20*, 20376−20386.
(10) Liu, W.; Miroshnichenko, A. E.; Neshev, D. N.; Kivshar, Y. S. *ACS Nano* **2012**, *6*, 5489−5497.
(11) Devilez, A.; Stout, B.; Bonod, N. *ACS Nano* **2010**, *4*, 3390−3396.
(12) Schuller, J. A.; Zia, R.; Taubner, T.; Brongersma, M. L. *Phys. Rev. Lett.* **2007**, *99*, 107401.
(13) Zhao, Q.; Zhou, J.; Zhang, F.; Lippens, D. *Mater. Today* **2009**, *12*, 60−69.
(14) Jylha, L.; Kolmakov, I.; Maslovski, S.; Tretyakov, S. *J. Appl. Phys.* **2006**, *99*, 043102.
(15) Kerker, M.; Wang, D.; Giles, C. *J. Opt. Soc. Am.* **1983**, *73*, 765−767.
(16) Bohren, C. F.; Huffmann, D. R. *Absorption and Scattering of Light by Small Particles*; Wiley: New York, 1983.
(17) García-Cámara, B.; Moreno, F.; González, F.; Saiz, J. M.; Videen, G. *J. Opt. Soc. Am. A* **2008**, *25*, 327−334.
(18) García-Cámara, B.; Alcaraz de la Osa, R.; Saiz, J. M.; González, F.; Moreno, F. *Opt. Lett.* **2011**, *36*, 728−730.
(19) García-Cámara, B.; María Saiz, J.; González, F.; Moreno, F. *Opt. Commun.* **2010**, *283*, 490−496.
(20) Nieto-Vesperinas, M.; Gómez-Medina, R.; Sáenz, J. J. *J. Opt. Soc. Am. A* **2011**, *28*, 54−60.
(21) Gómez-Medina, R.; García-Cámara, B.; Suárez-Lacalle, I.; González, F.; Moreno, F.; Nieto-Vesperinas, M.; Sáenz, J. J. *J. Nanophotonics* **2011**, *5*, 053512.
(22) García-Etxarri, A.; Gómez-Medina, R.; Froufe-Pérez, L. S.; López, C.; Chantada, L.; Scheffold, F.; Aizpurua, J.; Nieto-Vesperinas, M.; Sáenz, J. J. *Opt. Express* **2011**, *19*, 4815−4826.
(23) Kuznetsov, A. I.; Miroshnichenko, A. E.; Fu, Y. H.; Zhang, J.; Luk'yanchuk, B. *Sci. Rep.* **2012**, *2*, 492.
(24) Evlyukhin, A. B.; Novikov, S. M.; Zywietz, U.; Eriksen, R. L.; Reinhardt, C.; Bozhevolnyi, S. I.; Chichkov, B. N. *Nano Lett.* **2012**, *12*, 3749−3755.
(25) Wheeler, M. S.; Aitchison, J. S.; Chen, J. I. L.; Ozin, G. A.; Mojahedi, M. *Phys. Rev. B* **2009**, *79*, 073103.
(26) Geffrin, J.; García-Cámara, B.; Gómez-Medina, R.; Albella, P.; Froufe-Pérez, L.; Eyraud, C.; Litman, A.; Vaillon, R.; González, F.; Nieto-Vesperinas, M.; Sáenz, J.; Moreno, F. *Nat. Commun.* **2012**, *3*, 1171.
(27) Palik, E. D. *Handbook of Optical Constants of Solids*; Elsevier: San Diego, 1998; pp 429−443.
(28) Yablonovitch, E.; Gmitter, T.; Harbison, J.; Bhat, R. *Appl. Phys. Lett.* **1987**, *51*, 2222−2224.
(29) Demeester, P.; Pollentier, I.; Dedobbelaere, P.; Brys, C.; Van Daele, P. *Semicond. Sci. Technol.* **1993**, *8*, 1124−1135.
(30) Draine, B. T.; Flatau, P. J. *J. Opt. Soc. Am. A* **1994**, *11*, 1491−1499.
(31) Evlyukhin, A. B.; Reinhardt, C.; Seidel, A.; Luk'yanchuk, B. S.; Chichkov, B. N. *Phys. Rev. B* **2010**, *82*, 045404.
(32) Schmidt, M. K.; Esteban, R.; Sáenz, J. J.; Suárez-Lacalle, I.; Mackowski, S.; Aizpurua, J. *Opt. Express* **2012**, *20*, 13636−13650.
(33) Rolly, B.; Bebey, B.; Bidault, S.; Stout, B.; Bonod, N. *Phys. Rev. B* **2012**, *85*, 245432.
(34) Fu, Y. H.; Kuznetsov, A. I.; Miroshnichenko, A. E.; Yu, Y. F.; Luk'yanchuk, B. *Nat. Commun.* **2013**, *4*, 1527.

NOTE ADDED AFTER ASAP PUBLICATION

The Acknowledgments have been updated. The revised version was re-posted on March 13, 2013.

Demonstration of zero optical backscattering from single nanoparticles

Steven Person,[†] Manish Jain,[†] Zachary Lapin,[‡,†] Juan Jose Sáenz,[¶] Gary Wicks,[†] and Lukas Novotny[*,‡,†]

Institute of Optics, University of Rochester, ETH Zürich, Photonics Laboratory, and Departamento de Física de la Materia Condensada, Universidad Autónoma de Madrid

E-mail: lnovotny@ethz.ch

Supporting Information Available

Scattering properties of cylinders

Mie scattering theory is a complete solution to Maxwell's equations for the scattering properties of spherical particles in a uniform medium.[1] As particles begin to deviate from perfect spheres, using Mie theory to calculate the backscattering scattering efficiency becomes approximate. To fully explain the scattering properties of a cylinder an alternate simulation method must be used. For simulating the scattering properties of the GaAs cylinders we used a discrete dipole approximation (DDA) code, DDSCAT 7.2.2, written and made available by Bruce Draine and Piotr Flatau.[2,3] For

[†] Institute of Optics, University of Rochester, Rochester NY 14627

[‡]ETH Zürich, Photonics Laboratory, 8093 Zürich, Switzerland

[¶]Departamento de Física de la Materia Condensada, Instituto "Nicolás Cabrera" and Centro de Investigación en Física de la Materia Condensada (IFIMAC), Universidad Autónoma de Madrid, 28049-Madrid, Spain

the purpose of comparing to Mie theory, the geometry of a cylindrical scatterer will be described in terms of an effective radius and aspect ratio. The effective radius is the radius of a sphere which contains the equivalent volume of the cylinder. The effective radius,r_{eff}, is calculated as

$$r_{\text{eff}} = \left[\frac{3}{2}A_{\text{rat}}\right]^{\frac{1}{3}} r \tag{1}$$

where r is the radius of the cylinder and A_{rat} is the aspect ratio defined as

$$A_{\text{rat}} = \frac{\text{height}}{\text{diameter}} = \frac{\text{height}}{2r}. \tag{2}$$

Figure Figure 1(a) is a comparison of the backscattering efficiency (Q_{b}) of a GaAs sphere and cylinder with the same radius and effective radius, respectively, of 90 nm immersed in a uniform

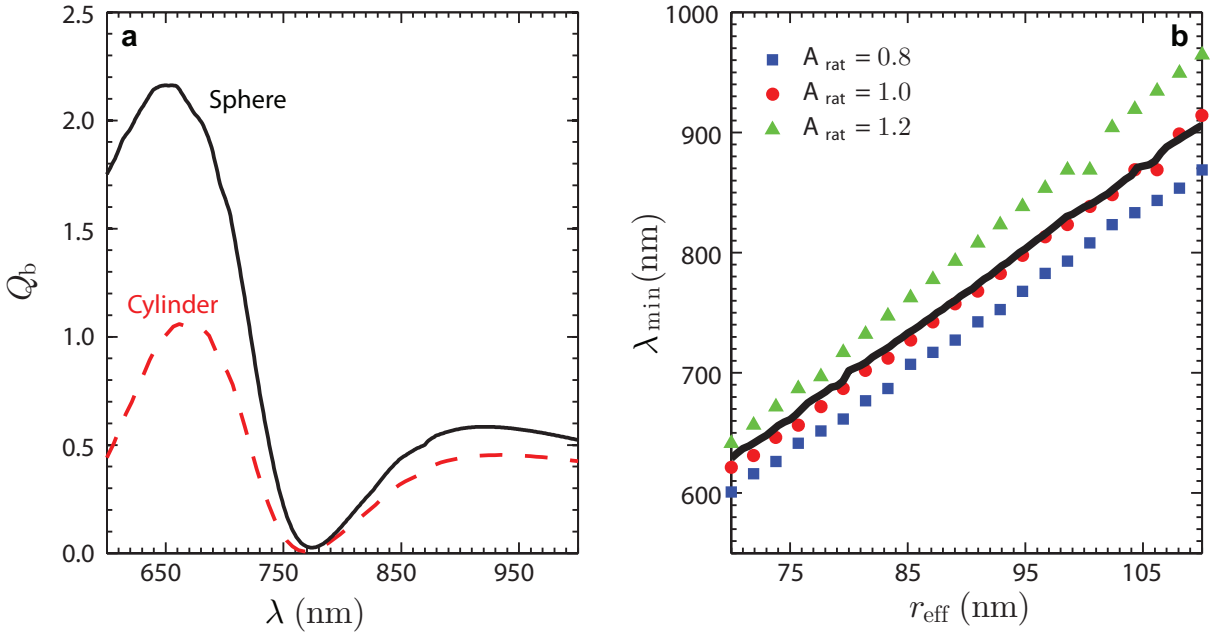

Figure 1: *Comparison of the scattering properties of a GaAs sphere and cylinder in a uniform medium of refractive index* $n_{\text{m}} = 1.47$. *(a) The backscattering efficiency* (Q_{b}) *of a GaAs sphere (solid) and cylinder (dashed) with the same effective radius of* $r_{\text{eff}} = 90$ *nm. (b) Dependence of the minimum* Q_{b} *location on* r_{eff} *for a GaAs sphere (solid line) and different aspect ratio* (A_{rat}) *cylinders (symbols).*

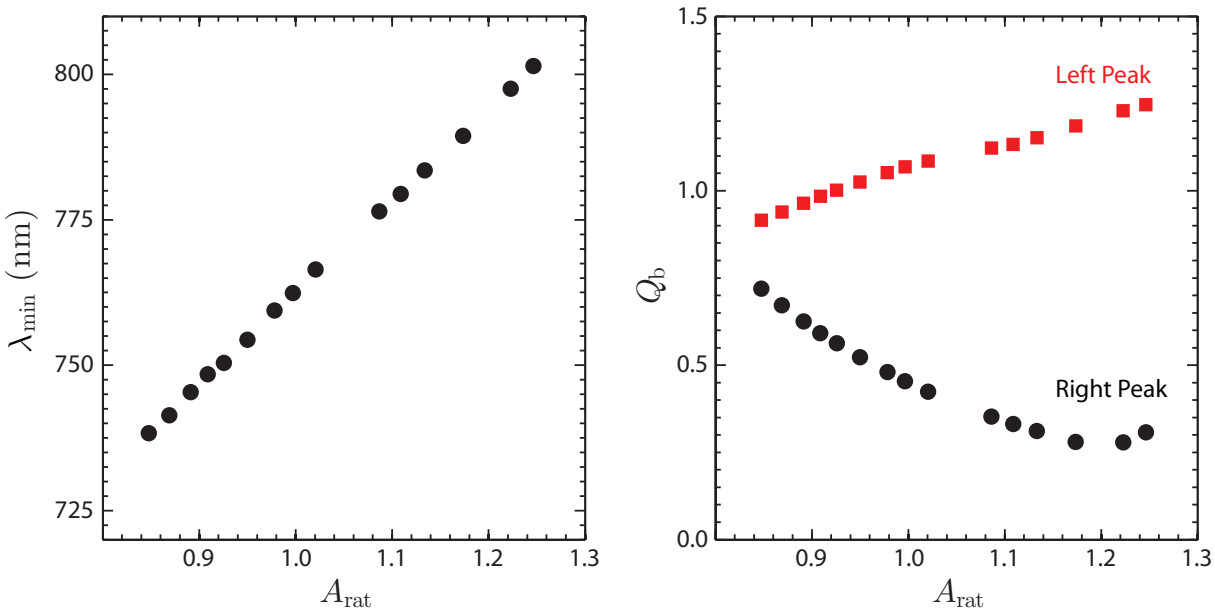

Figure 2: *Effect of aspect ratio on backscattering efficiency curve. (a) Shift in the location of the minimum backscattering efficiency (Q_b) for different aspect ratio (A_{rat}) cylinders with an effective radius, r_{eff} of 90 nm. (b) Change in the peak value of Q_b to the left (square) and right (circle) of the minimum within the simulated wavelength range.*

medium with refractive index, n_m=1.47. Mie theory is used for the sphere while DDA is used to compute the properties of the cylinder. The minimum in the backscattered field is located at the same wavelength for both structures, however, the peak at ∼650 nm is suppressed for the cylindrical scatterer. For an aspect ratio of 1 (circles), Fig. Figure 1(b) shows that the location (λ_{min}) of the minimum backscattering efficiency follows closely that of a sphere (solid curve). If the aspect ratio is increased(decreased) the minimum will red(blue) shift when compared to a sphere of the same volume but the trend of the minimum going to longer wavelengths for larger structures remains. The shift in the backscattering minimum location with aspect ratio is linear over the ±20% variation from unity simulated in Fig. Figure 2(a). Along with the shift in the minimum location, Fig. Figure 2(b) illustrates the asymmetry around the minimum also changes with the aspect ratio.

Control experiments with gold nanoparticles

To rule out any discrepancies due to a reflected field caused by the slight index mismatch between substrate and the immersion oil we have performed control experiments with gold nanoparticles. Spectra of 100nm diameter Au spheres with a similar substrate and index matching fluid were acquired. Figure Figure 3 shows the good agreement of an example spectra and Mie theory.

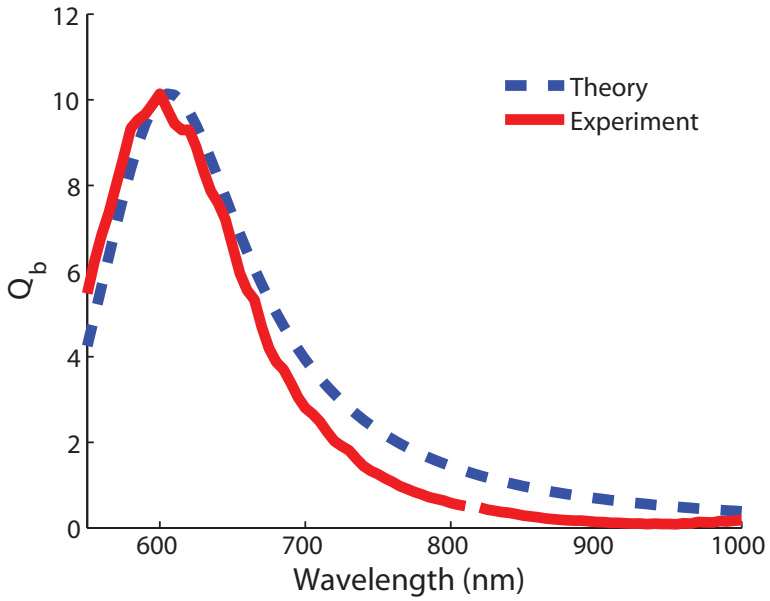

Figure 3: Backscattering of a 100 nm Au particle. Solid line is experimental measurements and dashed line is theoretical backscattering calculated with Mie scattering theory.

References

(1) Bohren, C. F.; Huffmann, D. R. *Absorption and Scattering of Light by Small Particles*; Wiley: New York, 1983.

(2) Draine, B. T.; Flatau, P. J. *J. Opt. Soc. Am. A* **1994**, *11*, 1491–1499.

(3) Draine, B.; Flatau, P. *arXiv:1202.3424 [physics.comp-ph]* **2012**.